

Quantum chaos

Giulio Casati

Dipartimento di Fisica, Università di Milano, Via Castelnovo—22100 Como, Italy and Istituto Nazionale di Fisica della Materia, Unita di Milano and INFN, sezione di Milano, Milano, Italy

(Received 22 February 1996; accepted for publication 20 June 1996)

In this paper we present an overview of important recent results in the study of a very controversial topic, the so-called quantum chaos. The theoretical and numerical results are compared with real laboratory experiments with special emphasis on the problem of ionization of hydrogen atoms in external microwave fields. © 1996 American Institute of Physics. [S1054-1500(96)01203-7]

The search for chaotic behavior in inherently quantum mechanical systems has been an area of considerable activity and interest recently. A potential case that is theoretically examined here is a simple kicked rotator. Although a classical kicked rotator displays chaotic behavior, it is shown that the quantum analog on average follows the classical chaotic motion only for relative short times. The possibility that similar behavior might be observable in a real system was explored by considering experimental results for hydrogen atom ionization in a microwave field. Although experiments results reported to date do not display chaotic behavior, it may be possible to tune conditions to observe chaos in this system.

I. INTRODUCTION

The modifications that quantum mechanics imposes on the general picture of classical chaos is a subject of growing interest for its theoretical relevance as well as for different physical applications. As a matter of fact the study of nonlinear dynamical systems has led to a much better understanding of the rich complexity of the classical motion. Of particular relevance was the discovery of the deterministic chaotic motion, which is a type of motion indistinguishable from a purely random motion, even if it is governed by strictly deterministic laws. This motion is characterized by exponential instability of orbits with respect to initial conditions, which leads to exponential loss of memory, decay of correlations, and approach to statistical equilibrium.

The reason why the exponentially unstable motion is called chaotic is in that almost all trajectories of such a motion are unpredictable in the following sense: according to the Alekseev–Brudno theorem¹ in the algorithmic theory of dynamical systems the information $I(t)$ associated with a segment of trajectory of length t is equal asymptotically to

$$\lim_{|t| \rightarrow \infty} \frac{I(t)}{|t|} = h, \quad (1)$$

where h is the so-called KS (after Kolmogorov–Sinai) entropy, which is positive for the exponentially unstable motion. This important result shows that in order to predict each new segment of a chaotic trajectory one needs additional information proportional to the length of this segment and independent of the full previous length of the trajectory. It means that this information cannot be extracted from the

observation of previous motion, even an infinitely long one! Notice that if the instability is not exponential but, for example, only a power law, then the required information per unit time decreases inversely proportional to the full previous length of trajectory and, asymptotically, the prediction becomes possible.

The exponential instability implies continuous spectrum of the motion, which, in turn, implies correlation decay; the latter property, which is called mixing in the ergodic theory, is essential for the validity of the statistical description. Indeed mixing provides the statistical independence of different parts (sufficiently separated in time) of a dynamical trajectory, and this is the main condition for the application of probability theory.

The mixing property implies the approach, on average, of any initially smooth distribution to a steady-state. This process is called *statistical relaxation*. The relaxation is, of course, time reversible, as is the motion along a particular trajectory. However, unlike the latter, the evolution of the distribution function is nonrecurrent. Notice that according to the Poincaré theorem the trajectory recurs infinitely many times, independently of the type of motion (regular or chaotic); the difference is that for regular motion the recurrence time is strictly bounded from above, whereas in the latter case arbitrarily large recurrence times are possible. The time reversibility of the distribution function is related to its very complicated structure, which becomes more and more “scarred” as the relaxation proceeds. In the case of the exponential instability of motion the spatial scale of the oscillations decreases also exponentially in time. It is in these fine spatial oscillations that the memory of the initial state is retained forever, and this is only possible in a continuous phase space.

However, the “true” mechanics of our world is quantum mechanics and therefore as far as the general problem of understanding the qualitative behavior of dynamical systems is concerned, we need to discover the extent at which the beautiful variety of classical chaotic motion persists at the microscopic level, in the domain of quantum mechanics. The interest of this problem lies in the foundations of quantum statistical mechanics as well as in several applications, like the distribution of nuclear and atomic energy levels, the interaction of atoms with electromagnetic fields, the problem of localization in disordered solids, the unimolecular reaction theory, etc.

Our intuition of quantum mechanics has been largely based on few exactly solvable models and on some approximate solutions of the Schrödinger equation. Since quantum mechanics is strictly connected to classical mechanics, one may wonder if quantum mechanics is richer than simple perturbative approaches may lead us to suspect. Preliminary investigations in this direction immediately unveiled a very-deep difficulty related to the fact that the energy and the frequency spectrum of any quantum motion, bounded in phase space, is always discrete. According to the existing theory of dynamical systems such motion corresponds to the limiting case of regular motion.

The prompt conclusion, out of this difficulty, would be the absence of any quantum chaos. For this reason it was even proposed the use of the term ‘‘quantum chaology,’’² which essentially means the study of the absence of chaos in quantum mechanics. If the above conclusion were true, a sharp contradiction would arise with the correspondence principle, which requires the transition from quantum to classical mechanics for all phenomena, including the new one: the dynamical chaos.

II. A MODEL OF QUANTUM CHAOS

In order to shed some light on the problem of quantum chaos, we start with a very simple dynamical system, which exhibits classical chaotic motion, and compare its classical and quantum evolution. It is very instructive to consider the following simple, periodically perturbed system, the so-called kicked rotator:

$$H = \frac{I^2}{2} + k \cos \vartheta \sum_{n=-\infty}^{\infty} \delta(t - nT). \quad (2)$$

This Hamiltonian describes a particle rotating on a ring with angular momentum I and subjected to periodic kicks of period T . Its dynamics is conveniently studied by looking at the map that describes the evolution over one period T . This map defines a canonical transformation of the phase space (I, ϑ) and is therefore area preserving. It is easy to see that the values $(\bar{I}, \bar{\vartheta})$ just after one kick are connected to the values (I, ϑ) after the previous kick, by the relation

$$\begin{aligned} \bar{I} &= I + k \sin \vartheta, \\ \bar{\vartheta} &= \vartheta + \bar{I}T. \end{aligned} \quad (3)$$

By iterating this map n times, we obtain the solution at time $t = nT$.

The map (3) is well known in the literature as the ‘‘standard map’’ or the ‘‘Chirikov map.’’ It has a very simple form but it contains most of the complexity of classical dynamical systems.³ Indeed for $k=0$ the system is integrable, $I = \text{const}$, and the orbits of the system in phase space are horizontal circles. When we turn on the perturbation, these invariant curves remain, albeit in distorted form, and are gradually destroyed by increasing the strength of the perturbation. These curves constitute impenetrable barriers for the orbits which means that the rotator energy remains confined in the vicinity of its initial value.

However, above a critical value, $kT \geq 1$ all invariant curves are destroyed. In such a situation two initially close orbits separate exponentially, the phases go rapidly random, and the angular momentum,

$$I_j = I_0 + k \sum_{n=0}^{j-1} \sin(\vartheta_n), \quad (4)$$

being a sum of random terms, performs a random-like walk. Indeed it can be shown³ that the momentum distribution function $f(I, \tau)$ of an ensemble of orbits at time τ (τ is the time measured in a number of kicks) is well approximated by a Fokker–Planck equation,

$$\frac{\partial f}{\partial \tau} = \frac{\partial}{\partial I} \left(\frac{1}{2} D \frac{\partial f}{\partial I} \right), \quad (5)$$

where the diffusion coefficient in the discrete time τ can be obtained from (4) in the random phase approximation

$$D = \frac{k^2}{2}. \quad (6)$$

Moreover, the ensemble average momentum \bar{I} grows linearly with time $\bar{I} \approx D\tau$. These qualitative predictions have been very well confirmed by numerical experiments.

We turn now to the quantum description of model (2), which is obtained from the quantization rule $I \rightarrow -i\hbar(\partial/\partial\vartheta)$. The quantum evolution is described by a unitary operator that maps the wave function $\psi(\vartheta)$ immediately after one kick to immediately after the next kick,

$$\bar{\psi}(\vartheta) = U\psi(\vartheta) = \exp(-i\hbar^{-1}k \cos \vartheta) \exp\left(i\hbar \frac{T}{2} \frac{\partial^2}{\partial \theta^2}\right) \psi(\theta). \quad (7)$$

The interesting point is how the quantum motion compares with the classical motion, especially in the regime $kT > 1$, where the classical motion is chaotic. As already mentioned, one of the most important features of classical chaotic motion is the exponential instability, which means that two initially close orbits separate exponentially with time. As a consequence, the *Ehrenfest time scale* τ_E , namely the time over which a minimum uncertainty packet follows a classical orbit, must be very short. Indeed, let us consider two orbits that are initially in a region of phase space of area \hbar . Their distance in phase, which at time $\tau=0$ is of order $\sqrt{\hbar}$, increases exponentially in time, namely $\delta\vartheta(\tau) \sim \hbar^{1/2} \exp(\lambda\tau)$, where λ is the so-called Lyapunov exponent. Then after a time $\tau_E \sim (1/2\lambda) \ln(1/\hbar)$ the distance $\delta\vartheta$ is comparable with the whole interval 2π , and therefore it is completely meaningless to compare the evolution of the quantum packet with the classical orbit. Therefore, for classically chaotic systems, the time τ_E is very short since it increases only logarithmically as $\hbar \rightarrow 0$ [Figs. 1(a)–1(c)].

What happens at later times? One may expect that the evolution of the quantum packet will reproduce somehow the evolution of the classical ensemble initially started in an area $\sim \hbar$ in phase space. In such a case the quantum excitation will mimic the classical, average, diffusive behavior. It was therefore a big surprise when, several years ago, it was

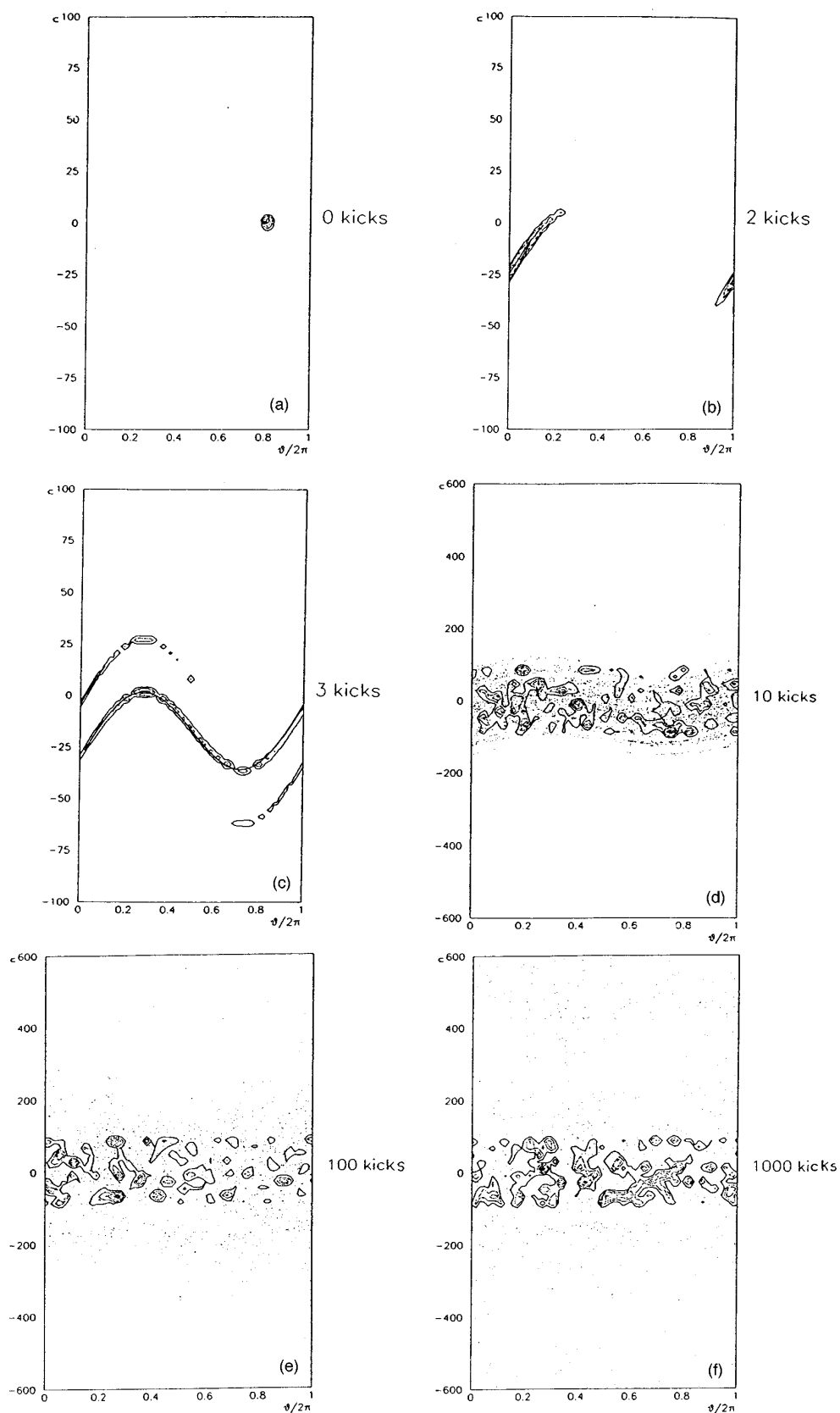


FIG. 1. A comparison between classical and quantum evolution in the kicked rotor for $K=5$, $k=25$, and $T=0.2$. The initial quantum state is a coherent packet. As to the classical evolution we considered 2000 trajectories starting in the same area, of size $\hbar (=1)$, occupied by the initial quantum state. In the following figures (b)–(f), the dots represent the classical trajectories while the curves are level curves of the Husimi distribution. For each figure, taken at different times, we divide by 8 the maximum value of the Husimi distribution and then plot the seven level curves. (b) $\tau=2$; (c) $\tau=3$; (d) $\tau=10$; (e) $\tau=100$; (f) $\tau=1000$. From this figure, as well as from Fig. 2, the quantum localization phenomenon is clearly evident.

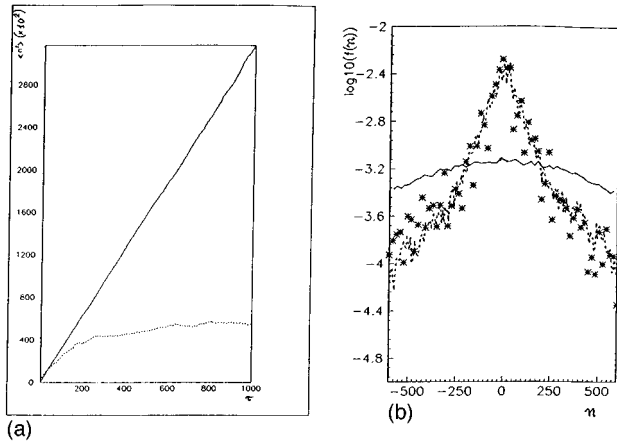


FIG. 2. Classical and quantum diffusion in the standard map for the same parameters of Fig. 1. (a) Classical (solid curve) and quantum (dotted curve) unperturbed energy $\langle n^2(\tau) \rangle = 2E$ as a function of time τ (number of map iterations). (b) Classical (solid curve) and quantum (dashed curve) probability distribution after time $\tau = 1000$. The stars give the Husimi distribution integrated over the angle ϑ .

found⁴ that the quantum motion mimics the classical one only up to a given time τ_D , while, for $\tau > \tau_D$, the quantum diffusive motion, unlike the classical, stops and enters a stationary oscillatory regime [Figs. 1(d)–1(f), Fig. 2].

We have now a quite satisfactory understanding of this phenomenon, even if a rigorous mathematical proof is still lacking. At the informal level one may say that, in the classical case, the evolution of the initial ensemble develops on separate independent orbits. In the quantum case instead, the different dynamical possibilities interfere, and this leads to the suppression of the diffusive process. A quantitative estimate of the *diffusive time scale* τ_D was obtained in Ref. 5 on the assumption that the quasienergy spectrum (i.e., the Floquet spectrum) is discrete. The idea is that according to Heisenberg uncertainty relations the quantum motion follows, on average, the classical motion up to a time of the order of the inverse of the average quasienergy levels spacing. This estimate gives⁵ $\tau_D \approx D/\hbar^2$.

To summarize, for classically chaotic systems, a coherent state follows a classical orbit only for a very short time $\tau_E \sim \ln(1/\hbar)$. For $\tau_E < \tau < \tau_D$ the quantum motion follows the classical only in the average. The diffusive time τ_D is much larger than τ_E and grows to infinity as $1/\hbar^2$. For $\tau \geq \tau_D$ the system reaches a steady state characterized by the momentum probability distribution [Fig. 2(b)],

$$f(n) \approx \frac{1}{l} \exp\left(-\frac{2|n - n_0|}{l}\right).$$

To be more precise, it is necessary to mention that the above is the “typical” behavior. For particular, resonant values of period T the behavior is completely different. Indeed it can be shown that if T is a rational multiple of $4\pi/\hbar$ then the quantum rotator energy increases like t^2 . However this exceptional, resonant behavior is a quantum phenomenon and has no classical analog.

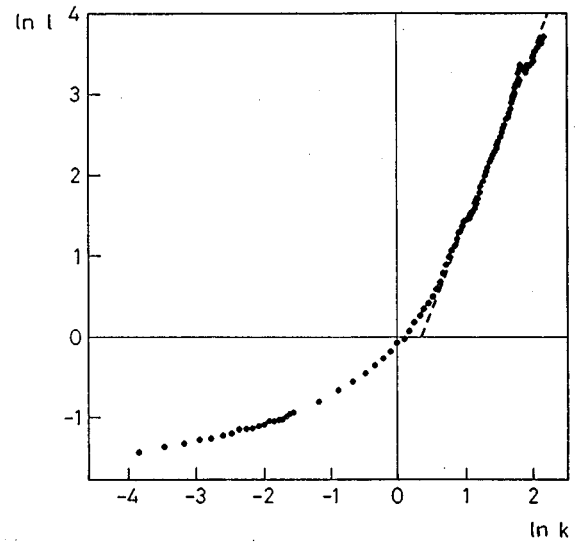


FIG. 3. Localization length l of the stationary distribution as a function of the parameter k . The dots are obtained from the numerical integration of the quantum map. Each dot gives the average value of $\ln l$ over 11 different very close values of k . The dashed line is the theoretical estimate $l = k^2/2$ obtained in the localization regime ($k \geq 1$). In the perturbative regime $k < 1$, a fitting of numerical data gives $l = \alpha/|\ln \beta k|$ with $\alpha \approx 1.11$, $\beta = 0.29$.

We would like to remark also that the *dynamical* localization must not be confused with the *perturbative* localization. Indeed, as is well known, in the perturbative regime, for small k , the population $P(m)$ on unperturbed states m corresponds to exponential distribution with localization length $l \sim 1/|\ln k|$. This has to be compared with dynamical localization in which $l \sim D \sim k^2/2$. A numerical check is presented in Fig. 3.

We think that the conception of characteristic time scales of quantum dynamics is a satisfactory resolution of the apparent contradiction, with the correspondence principle mentioned in the Introduction. Some physicists, however, feel that such an explanation is, at least, ambiguous because it includes two limits that do not commute:

$$\lim_{|t| \rightarrow \infty} \lim_{\hbar \rightarrow \infty} \neq \lim_{\hbar \rightarrow \infty} \lim_{|t| \rightarrow \infty}.$$

While the first order leads to the classical chaos, the second one results in an essentially quantum behavior with no chaos at all. The general structure of quantum dynamics on the plane (\hbar, t) is outlined in Fig. 4.

The limit $|t| \rightarrow \infty$ is related to the existing ergodic theory, which is asymptotic in t . Meanwhile the new phenomenon of quantum chaos requires the modification of the theory to a finite time, which is a difficult mathematical problem still to be solved. On the other hand, the practical importance of statistical laws even for a finite time interval is in that they provide a relatively simple description of the *essential* behavior for a very complicated dynamics.

In any event, if quantum mechanics is the universal theory, as commonly accepted, then the phenomenon of the “true” (classical-like) dynamical chaos, strictly speaking,

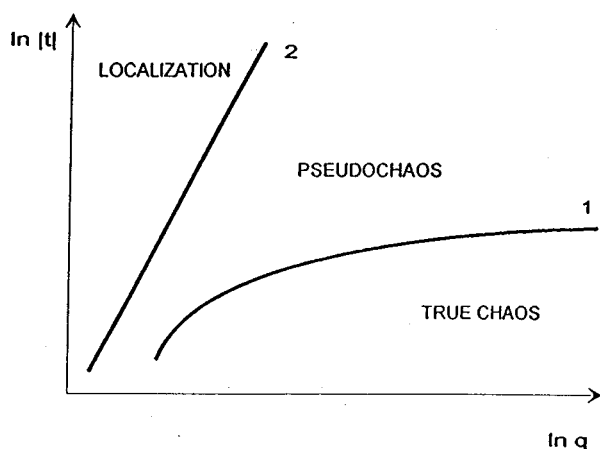


FIG. 4. Time scales of classically chaotic quantum motion: curve 1—random time scale $\tau_E \sim \ln q$; curve 2—relaxation time scale $\tau_D \sim q^a$; $q \gg 1$ is the quasiclassical parameter.

does not exist in nature. Nevertheless, the conception of “true” chaos is very important in the theory as the limiting pattern to compare with the real quantum chaos.

III. EXPERIMENTAL EVIDENCE

The next question now is whether the interesting phenomena described above are a general occurrence in quantum mechanics and not a peculiar property of the particular model chosen, namely the kicked rotator. Another interesting question is whether or not the quantum suppression of classical chaotic diffusion can be observed in real laboratory experiments.

One of the most significant cases where classical and quantum chaos confronted each other was in the explanation of an experiment on Hydrogen atoms, first performed in 1974 by Bayfield and Koch.⁶ Single atoms prepared in very elongated states with high principal quantum number ($n_0 \approx 63-69$) were injected into a microwave cavity and the ionization rate was measured. The microwave frequency was 9.9 GHz, corresponding to a photon’s energy well below the ionization energy of level 66 and even lower than the transition from state 66 to 67. Much surprise therefore followed the discovery that a very efficient ionization occurred when the electric field intensity exceeded a threshold value of about 20 V/cm (for $n_0=66$), much lower than the static Stark value. More surprisingly, a numerical simulation⁷ showed that classical mechanics could reproduce quite well the experimental data. The subsequent analysis,⁸ still in classical terms, of a related model of an electron trapped by the image charge on liquid helium, explained the threshold intensities as critical values for the onset of chaotic diffusion in action space. A condition for the occurrence of full chaotic diffusion is that the microwave frequency is greater than the frequency of the electron’s motion, namely $\omega n_0^3 > 1$. However, the hydrogen atom is a quantum object: The quantum mechanical evolution was investigated in the one-dimensional approximation,⁹ and for $\omega n_0^3 > 1$ was predicted an ionization

threshold higher than the classical value, to overcome the occurrence of quantum localization. This effect vanishes while approaching the main resonant region $\omega n_0^3 \approx 1$, and this may explain why classical mechanics works so well at lower values of ωn_0^3 .

The dimensionless classical Hamiltonian for a hydrogen atom interacting with a time-periodic microwave field in the dipole approximation is

$$H(z, p, t) = \frac{p^2}{2} - \frac{1}{r} + \epsilon z \cos(\omega t) \quad (z \geq 0). \quad (8)$$

The unperturbed Hamiltonian describes both bounded (with negative energy) and unbounded motions. As it was shown in Ref. 10 the main qualitative features of the motion are given by the one-dimensional model; moreover, since we are interested in exploring the dynamics that precedes ionization, we confine to negative energies, and introduce accordingly action-angle variables (n, θ) , thus obtaining

$$H = -\frac{1}{2n^2} + \epsilon z(n, \theta) \cos \omega t. \quad (9)$$

By integrating the equations of motion over one period of the unperturbed orbit, in first order in ϵ , we obtain an approximate map for the canonical variables (ν, ϕ) , where $\nu = E/\omega = -1/2n^2\omega$ is the number of photons exchanged by the atom with the field and ϕ is the field phase at perihelion.¹⁰

A linearization of the map around the initial value $\nu_0 = -1/2n_0^2\omega$ yields, once again the Standard map:¹⁰

$$\begin{aligned} \bar{\nu} &= \nu + k \sin \phi, \\ \bar{\phi} &= \phi + T\bar{\nu}, \end{aligned} \quad (10)$$

where $k \approx 2.6\epsilon/\omega^{5/3}$ and $T = 6\pi\omega^2 n_0^5$.

In spite of the various simplifications so far introduced, the map (10) still gives a good description of the mean behavior of the system and allows interesting conclusions. Indeed, the condition $kT \approx 1$ gives the threshold for transition to classical chaos leading to fast ionization:

$$\epsilon_c \approx \frac{1}{50n_0^5\omega^{1/3}}. \quad (11)$$

In the corresponding quantum model we expect similarly to the kicked rotator, exponential localization of the wave function in ν . After the relaxation time τ_D the system reaches the steady state

$$g(\nu) \approx \frac{1}{l_s} \exp\left(-2 \frac{|\nu - \nu_0|}{l_s}\right), \quad (12)$$

where the predicted localization length in the number of photons is

$$l_s \approx \frac{k^2}{2} \approx 3.3\epsilon^2\omega^{-10/3},$$

and equals the diffusion coefficient in ν space. If l_s is greater than the number of photons required to ionize the atom

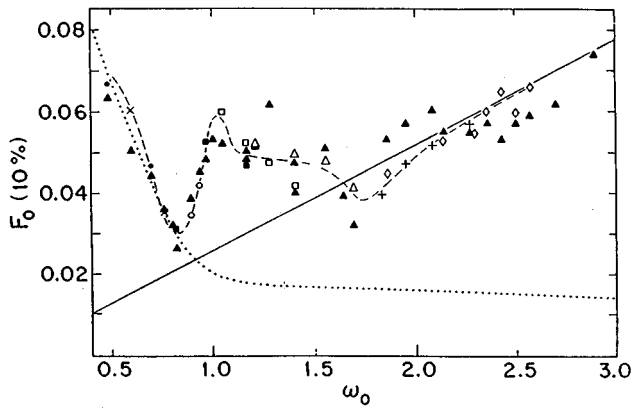


FIG. 5. A comparison at identical parameter values of experimental and quantum-mechanical values for the microwave field strength for 10% ionization probability, as a function of microwave frequency. The field and frequency are classically scaled, $\omega_0 = n_0^3 \omega$ and $\epsilon_0 = n_0^4 \epsilon$. Ionization includes excitation to states with n above \bar{n} . The theoretical points are shown as solid triangles. The dashed curve is the one drawn through the entire experimental data set shown in Fig. 2. Values of n_0, \bar{n} are \bullet , 64, 114; \times , 68, 114; \circ , 71, 114; \square , 76, 114; \square , 80, 120; \triangle , 86, 130; $+$, 94, 130; \diamond , 98, 130. Multiple theoretical values at the same ω_0 are for different compensating experimental choices of n_0 and ω . The dotted curve is the classical chaos border. The solid line is the quantum 10% threshold according to localization theory for the present experimental conditions.

$l_s \geq (2\omega n_0^2)^{-1}$, then localization cannot prevent ionization. This condition leads to the *quantum delocalization border*,

$$\epsilon_q \approx 0.4\omega^{7/6}n_0^{-1}. \quad (13)$$

Unexpected though these predictions may have been at their first appearance,^{9,10} they were confirmed by recent experimental results on the microwave ionization of hydrogen atoms.^{11,12} It was found that experimental and numerical data fairly well agree with localization theory and at the same time appreciably deviate from classical predictions (Fig. 5).

The experiments described in Ref. 12 were precisely designed for the purpose of checking localization theory; as a matter of fact, special care was taken in order that numerical computations could simulate as closely as possible the experimental conditions. Therefore, they provide experimental evidence of the quantum suppression of the classically chaotic diffusion due to the localization phenomenon.

IV. STABILITY OF HYDROGEN ATOM IN STRONG EXTERNAL DRIVING FIELD: THE MAGIC MOUNTAIN

From the theoretical and experimental results presented in Fig. 5 one naturally expects that by increasing the intensity of the external field a larger and larger fraction of the atoms will be ionized until complete ionization takes place. By further increasing the field one expects this process to be even faster. However strange it may seem, this expectation turns out to be false! A careful analysis of the classical motion shows that at very high field values the atoms become stable again. For details we refer to original papers¹³⁻¹⁵ (see also Ref. 16). It is, however, instructive to present an intuitive

explanation of this apparent paradoxical result. If one rewrites the Hamiltonian (8) in cylindrical coordinates one obtains

$$H = \frac{p_z^2}{2} + \frac{p_\varrho^2}{2} + \frac{m^2}{2\varrho^2} - \frac{1}{\sqrt{\varrho^2 + z^2}} + \epsilon z \cos \omega t, \quad (14)$$

where z is the direction of the linearly polarized external field and m is the projection of the angular momentum on the field direction. For large values of ϵ and ϱ , the z motion is dominated by the driving field $z \sim (\epsilon/\omega^2)\cos \omega t$. One can then perform an average over the z motion and look on the ϱ motion, which will be described by the average Hamiltonian,

$$\bar{H} = \frac{p_\varrho^2}{2} + \frac{m^2}{2\varrho^2} + \frac{2\omega^2}{\pi\epsilon} \ln\left(\frac{\varrho\omega^2}{\epsilon}\right). \quad (15)$$

The position of the minimum of the potential in (15) increases with the field; the physical reason is quite clear: the large amplitude of field oscillations leads to a decrease of the attractive Coulomb force while the centrifugal potential remains the same. Obviously the averaged Hamiltonian (15) gives a good description of the real three-dimensional (3-D) motion if the frequency $\Omega \sim \omega^2/\epsilon m$ of the oscillations in ϱ is much less than the external frequency $\Omega \ll \omega$. This condition leads to the stabilization border

$$\epsilon > \epsilon_{\text{stab}} = \delta \frac{\omega}{m}, \quad (16)$$

where δ is a numerical constant. In order to check the above estimates we investigated the process of ionization of the classical atom by numerical solution of the exact Hamiltonian system (14). The initial distribution of classical trajectories was chosen to model a quantum state with fixed values of principal quantum number n_0 (action), orbital momentum l , and its projection on the field direction m (magnetic quantum number). Therefore the classical trajectories had the same initial value of n, l, m , and the phases conjugated to n and l were homogeneously distributed in the interval $[0, 2\pi]$. The field was smoothly switched on and off during a number of field periods $T_{\text{sw}} = \omega_0$, and the total interaction time (number of field periods) was chosen as $T_{\text{int}} = 500\omega_0$ (so that the physical interaction time was always fixed and equal to 500 unperturbed periods of the electron). Different values of ω_0 were considered, from $\omega_0 = 1$ up to $\omega_0 = 30$. We numerically investigated the dependence of the ionization probability W_{ion} (or stabilization probability $W_{\text{stab}} = 1 - W_{\text{ion}}$) on the field strength ϵ . The ionization probability W_{ion} was determined as the relative number of trajectories with positive energy after the field pulse (the total number of trajectories for each run was taken equal to 100). The numerical results for W_{stab} are presented in Fig. 6. The most remarkable fact is the appearance of a large fraction of nonionized trajectories with increasing field intensity.

Notice that the stabilization border (16) is relevant only if $\omega m^3 < 3$. Indeed, in the opposite case the electron passes sufficiently far from the nucleus and the change of energy during these passages are exponentially small and atoms remain stable up to very high fields.^{13,14} This fact is in agree-

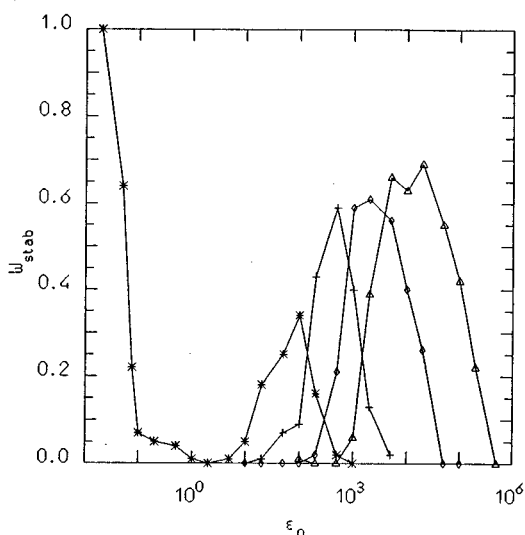


FIG. 6. Dependence of stabilization probability W_{stab} ($W_{\text{stab}}=1-W_{\text{ion}}$) on field strength ϵ_0 for $\omega_0=1$ (*), 3(+), 10(\diamond), and 100(\triangle) with initial values $m/n=0.25$, $l/n=0.3$. The interaction time is equal to $500\omega_0$ field periods. (Sets of numerical points are joined by segments to guide the eye.) For the case $\omega_0=1$ we have computed W_{stab} also for small ϵ_0 down to the chaos border.

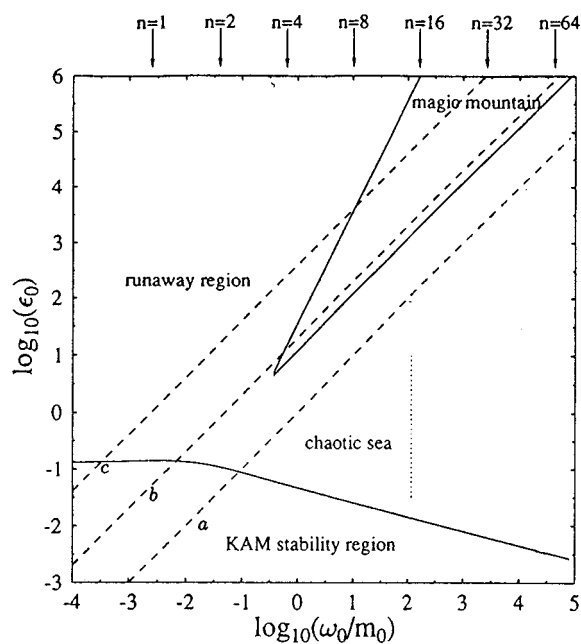


FIG. 7. The stability borders for Hamiltonian (1) at fixed $\omega=0.001$ and $m=0.4$. The lower curve is the usual chaos border $\epsilon_0 \approx 1/50\omega_0^{1/3} = 1/50(\omega m^3)^{1/2}(m_0/\omega_0)^{1/4}$. For small ω_0 this border approaches the usual static border $\epsilon_0 \approx 0.13$. The "magic mountain" of stability is delimited from below by the stabilization border $\epsilon_0 \approx 12(\omega_0/m_0)$ and from above by the destabilization border $\epsilon_0 \approx (16L/\pi)(\omega_0/m_0)^2$ with $L = \ln(\sqrt{2/e}\pi(\sqrt{\epsilon_0/\omega_0 m_0}))$. The border below which the Kepler map description is valid is given, in the present case, with fixed m and ω , by the line $\epsilon_0 = 0.2(\omega_0/m_0)$ (not drawn in the figure). The present picture is drawn at fixed ω and m . If instead we keep n_0 fixed, then the system will always be stable in the region to the right of the dotted vertical line given by $\omega_0 m_0^2 = 3$.

ment with the numerical simulations. In Fig. 7 we present a general picture of the stability diagram in the $(\epsilon_0, \omega_0/m_0)$ plane. The most impressive result of our analysis is the "magic mountain" of stability in the upper rightmost part of the figure that emerges from the chaotic sea and, coming from infinity, approaches, but does not touch, the familiar territory of KAM stability. The latter is delimited by the full curve in the lower part of Fig. 7. Quite obviously the details of the classical motion depend separately on all parameters m, ϵ, ω , as well as on the initial conditions, however Fig. 7 gives the correct main qualitative behavior.

One of the important conclusions of our investigations is that stabilization can be obtained not only when the size of the electron oscillations $\alpha = \epsilon/\omega^2$ is larger than the size of the atom $2n_0^2$, but also in the other limiting case when $\alpha \ll n_0^2$. Our conclusion differs from other results¹⁷ in which stabilization is predicted to occur only when α is larger than the size of the atom. Also, a condition considered as necessary for stabilization is that the external frequency is larger than ionization energy. According to our results stabilization takes place even for $\hbar\omega_0$ much less than the coupling energy.

A point we would like to stress is that the Rydberg stabilization presented here is a very interesting phenomenon, which we consider more important than the stabilization of atoms in very strong fields, with field strength and frequency larger than the corresponding atomic values ($\epsilon, \omega \gg 1$). The reason is that in such large fields the ground state is strongly modified and therefore the frequency of transitions between states of a stabilized atom cannot be larger than the atomic unit of energy. Instead, in the case of Rydberg stabilization, the field, which is strong enough to stabilize the Rydberg state, does not modify the ground state, since $\epsilon \ll 1$, $\omega \ll 1$, and it acts as a small perturbation. Therefore the electron energy in the ground state remains approximately the same as for the unperturbed atom while in the Rydberg stabilized state the electron energy can be very high due to fast oscillations in the driving field. Indeed the difference in energy between these two states is of the order of ϵ^2/ω^2 . For example, for a CO₂ laser with $\omega \approx 1/300$ (0.1 eV) stabilization of the Rydberg state with $n_0=40$, $m=2$ takes place for $\epsilon \sim 2 \times 10^8$ V/cm and the transition frequency between the stabilized Rydberg state and the ground state is ~ 1000 eV. It would be very important to estimate the transition rate for the above radiative process. However, we think that this rate will be comparable with the transition rate in the normal Rydberg atom, since the size of the atom is the same as for the unperturbed Rydberg state $\alpha = \epsilon/\omega^2 \approx 2n_0^2$.

The possibility of radiation of photons with very high energy makes Rydberg stabilization a very interesting phenomenon.

V. CONCLUSION: SOME RANDOM REMARKS ON QUANTUM CHAOS

So far there is no common agreement, even among physicists, as to the definition of quantum chaos. The classical-like definition related to the exponential instability is completely not adequate since such chaos is possible only

in very exotic examples and does not describe the typical quantum behavior. On the other hand, the most popular definition, as some specific quantum properties for classically chaotic systems, seems to us also unacceptable (and even somewhat helpless) from the physical point of view. For example, such a “chaos” may happen to be a perfectly regular motion in the case of perturbative localization discussed in this paper.

It is quite natural in physics, unlike mathematics, first to study a new phenomenon, like dynamical chaos and only at a later stage, after understanding it sufficiently, to try to classify it, to find its proper place in the existing theories and eventually to choose the most reasonable definition.

In attempts to construct such a reasonable definition of quantum chaos, we would like to emphasize the most striking peculiarity of this phenomenon as discussed above, namely that all statistical properties of classical dynamical chaos are present in quantum dynamics but only within restricted and different time scales. Therefore quantum chaos is “*finite-time* dynamical chaos.” It is a new phenomenon that reveals the intrinsic complexity and richness of the motion with a discrete spectrum (which has been considered since long ago as the most simple and regular). This is true also for classical linear waves, but the linearity of quantum equations is not an approximation as in classical physics but a fundamental and universal physical property.

The practical importance of statistical laws, even for a finite time interval, is in that they provide a relatively simple description of the *essential* behavior for a very complicated dynamics. The existing ergodic theory of dynamical systems that is asymptotic in time looks inadequate to properly describe this new phenomenon. A new ergodic theory is required that could analyze the finite time statistical properties of dynamical systems.

Also, we would like to make a few comments on the problem of quantum measurement. The studies in quantum chaos suggest that it may have a close relation to this problem. First the measurement device is by purpose a macroscopic system for which the classical description is a very good approximation. In such a system the true chaos with exponential instability is quite possible. The chaos in the measurement classical device is not only possible but unavoidable since the measurement system has to be, by purpose again, a highly unstable system; indeed, a microscopic

intervention produces here the macroscopic effect. The importance of chaos for the quantum measurement is in that it destroys the coherence of the initial pure quantum state to be measured converting it into the incoherent mixture. In the existing theories of the quantum measurement this is described as the effect of the external noise.¹⁸ The chaos theory allows to get rid of the unsatisfactory effect of the external noise and to develop a purely dynamical theory for the loss of quantum coherence.¹⁹ Unfortunately this is not yet the whole story. Indeed, besides the loss of coherence the most important effect of the quantum measurement is the redistribution of probabilities $|\psi|^2$ according to the result of the measurement, the famous ψ -collapse, which remains to be explained. It seems that any dynamical explanation of the ψ -collapse requires some changes in the existing quantum mechanics and this is the main difficulty both technical and philosophical.

¹V. M. Alekseev and M. V. Yakobson, Phys. Rep. **75**, 287 (1981).

²M. Berry, Proc. R. Soc. London, Ser. A **413**, 183 (1987).

³B. V. Chirikov, Phys. Rep. **52**, 623 (1979).

⁴G. Casati, B. V. Chirikov, J. Ford, and F. M. Izrailev, in *Stochastic Behavior in Classical and Quantum Hamiltonian Systems*, Lecture Notes in Physics, edited by G. Casati and J. Ford (Springer-Verlag, Berlin, 1979), Vol. 93, p. 334.

⁵B. V. Chirikov, F. M. Izrailev, and D. L. Shepelyansky, Sov. Sci. Rev. Sec. C **2**, 209 (1981).

⁶J. E. Bayfield and P. M. Koch, Phys. Rev. Lett. **33**, 258 (1974).

⁷J. C. Leopold and I. C. Percival, Phys. Rev. Lett. **41**, 944 (1978).

⁸R. Jensen, Phys. Rev. Lett. **49**, 1365 (1982); Phys. Rev. A **30**, 386 (1984); N. B. Delone, B. P. Krainov, and D. L. Shepelyansky, Sov. Phys. Usp. **26**, 551 (1983).

⁹G. Casati, B. V. Chirikov, and D. L. Shepelyansky, Phys. Rev. Lett. **53**, 2525 (1984).

¹⁰G. Casati, B. V. Chirikov, I. Guarneri, and D. L. Shepelyansky, Phys. Rep. **54**, 77 (1987); G. Casati, I. Guarneri, and D. L. Shepelyansky, IEEE J. Quantum Electron. **QE-24**, 1420 (1988).

¹¹E. J. Galvez, B. E. Sauer, L. Moorman, P. M. Koch, and D. Richards, Phys. Rev. Lett. **61**, 2011 (1988).

¹²J. E. Bayfield, G. Casati, J. Guarneri, and D. W. Sokol, Phys. Rev. Lett. **63**, 364 (1989).

¹³F. Benvenuto, G. Casati, and D. L. Shepelyansky, Phys. Rev. A **47**, R786 (1993).

¹⁴F. Benvenuto, G. Casati, and D. L. Shepelyansky, Zeit. Phys. B **94**, 481 (1994).

¹⁵G. Casati, I. Guarneri, and G. Mantica, Phys. Rev. A **50**, 5018 (1994).

¹⁶R. V. Jensen and B. Sundaram, Phys. Rev. A **47**, R778 (1993).

¹⁷R. J. Vos and M. Gavrilu, Phys. Rev. Lett. **68**, 170 (1992).

¹⁸J. A. Wheeler and W. H. Zurek, *Quantum Theory and Measurement* (Princeton University Press, Princeton 1983).

¹⁹M. Namiki and S. Pascazio, Phys. Rep. **232**, 301 (1993).